



Finite element-based optimization of wind turbine blade twist for balanced aerodynamic efficiency and structural integrity

Syed Assiqul Haque¹, Samin Abrar Chowdhury¹, Kazi Naimul Hoque^{1,*}

ARTICLE INFO

Article history:

Received 12 Jul 2024;
in revised from 16 Jul 2024;
accepted 24 Jul 2024.

Keywords:

Wind turbine blade, aerodynamic efficiency, structural integrity, twisting angle optimization, composite materials, finite element analysis.

ABSTRACT

The aerodynamic efficiency of a wind turbine is reliant on the design of its blades. To maximize wind energy conversion, the turbine blades must be positioned at the optimal angle to face the oncoming wind throughout their length. This is achieved through blade twisting. However, while increasing the twist angle can enhance power output, it may compromise structural integrity. This paper presents the optimization process for the twisting angle of a horizontal axis wind turbine (HAWT) model, focusing on structural integrity and power output. An iterative design-based optimization approach, utilizing Finite Element modeling under static load, is employed to ensure structural strength. A direct analysis method is employed to optimize the twisting angle for power output. The NACA 2412 airfoil is selected for blade design using SolidWorks. Structural analysis of various twisted HAWT blade models is conducted in ANSYS Mechanical and QBlade software. The twisting angle derived from structural analysis is then compared with the twisting angle obtained from power output analysis to determine the final twisted model that meets both criteria.

© SECMAR | All rights reserved

1. Introduction.

A wind turbine blade is a crucial component in the energy production process, as it efficiently converts the kinetic energy of wind into useful power through its rotating blades. Ensuring maximum aerodynamic efficiency is key, and this is influenced by the structural integrity of the rotor blades and their ability to harness the maximum wind energy [1, 2].

To ensure the structural integrity of Horizontal Axis Wind Turbine (HAWT) blades, it is important to guarantee a long and maintenance-free life cycle, stiffness, fatigue resistance, and high strength while maintaining an aerodynamically thin and lightweight structure. While conventional materials like structural steel and other metals can meet some of these requirements, alternate materials such as Carbon and Glass fiber-based composite structures have been identified in published works [2, 3]. To harness wind energy efficiently, the turbine blade

must meet the wind at the correct angle. As a result, HAWT blades are designed to be twisted at certain angles, enabling them to capture 5-10% more energy from the wind and to function efficiently in areas with lower wind speeds [4].

Hoque et al. conducted a comprehensive analysis of wind turbine blades made from various composite materials, comparing their performance to traditional structural steel [3]. The blades were designed using the NACA 2412 airfoil section with no twisting angle, and structural analysis was performed using FEA on six different materials. Additionally, nodal analysis was carried out to identify maximum stress and deformation locations. The results indicated that Epoxy E-glass UD, Epoxy S-Glass UD, and Epoxy Carbon UD (230 GPa) Prepreg were significantly superior to the other materials tested.

Liu et al. investigated the optimization of wind turbine blades for fixed-pitch fixed-speed (FPFS) horizontal-axis wind turbine by linearizing the blade chord and twisting angle profiles [5]. This novel method aimed to maximize the annual energy production for a specific wind speed distribution. By comparing it with the preliminary blade design, it was found that this method enhances the power performance while reducing

¹Bangladesh University of Engineering and Technology.

*Corresponding author: Kazi Naimul Hoque. E-mail Address: kazi-naim@name.buet.ac.bd.

the manufacturing cost and applicable for any new FPFS blade design.

Alaskari et al. examined the influence of various design parameters on wind turbine blades using QBlade software, which applies the blade element momentum method [6]. For their study, they utilized the SG6043 airfoil, with the blades measuring 1.17m in length [6]. The outcome showed that the optimized blade improved the performance of the blade and the result from the software was of high accuracy and thus showed the reliability and user friendliness of QBlade software in the field of wind turbine blade.

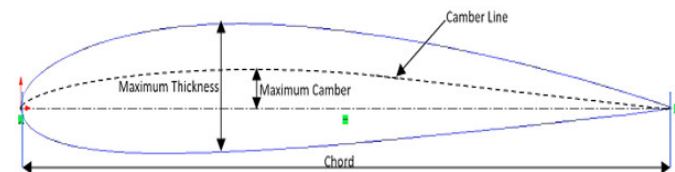
Mendez and Greiner presented a method using genetic algorithms to optimize the wind turbine blade chord and twisting angle to maximize the power output for a specific Weibull wind distribution [7]. The Blade Element Theory is employed and validated against experimental data from the Risø test turbine. The result showed improved performance at lower wind speed but slightly worse performance at higher wind speed. However, the optimized blade shows increased annual energy production than the original blade.

The optimization process of twisting angles presents two key challenges. The first challenge is to determine the optimum twisting angle distribution of the blade. Given the numerous combinations of twisting angles possible, an iterative design approach is crucial. These twisted models are designed using SolidWorks and analyzed using the Finite Element Analysis (FEA) package ANSYS Mechanical to find the optimum model in terms of structural strength. The second challenge is to determine the power output for different twisted models, necessitating a second iterative method. The designed models are imported into QBlade software to analyze their power output for different twisted models.

2. Blade Geometry.

The blade shape has been designed to align with previous work [3]. Hoque et al. conducted an analysis of wind turbine blades using various composite materials and employed the NACA 2412 airfoil section for the design of a blade with zero twist angle. Therefore, for this study, the primary blade shape was developed based on the NACA 2412 airfoil section [3]. The shape of the NACA 2412 airfoil section is illustrated in Fig. 1.

Figure 1: NACA 2412 airfoil section.

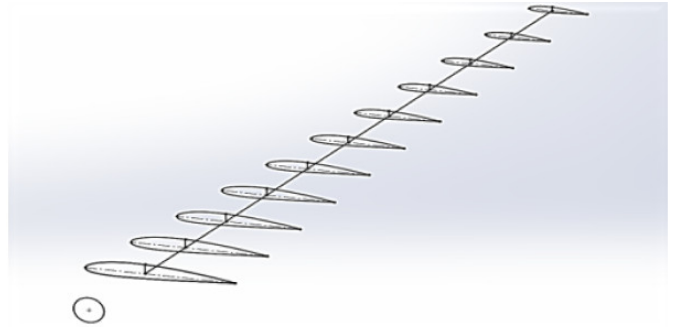


Source: Authors.

The whole blade is designed with ten equally spaced NACA profiles as shown in Fig. 2 for the implementation of twisting angle. Fig. 3 represents the rendered model of the primary

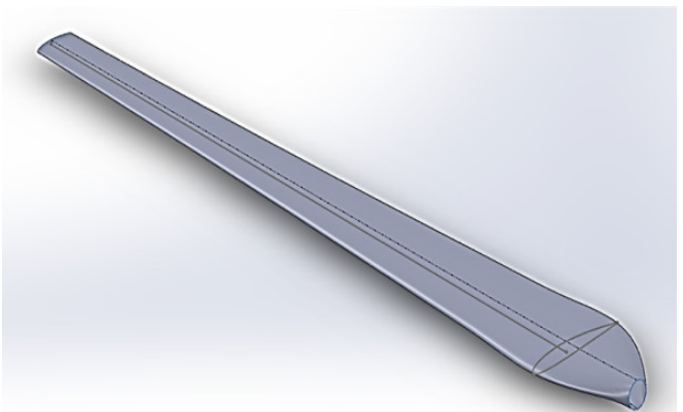
blade design without twisting angle. All the required design parameters are provided in Table 1.

Figure 2: Blade segmentation.



Source: Authors.

Figure 3: Primary blade model without twisting.



Source: Authors.

Table 1: Blade properties [3].

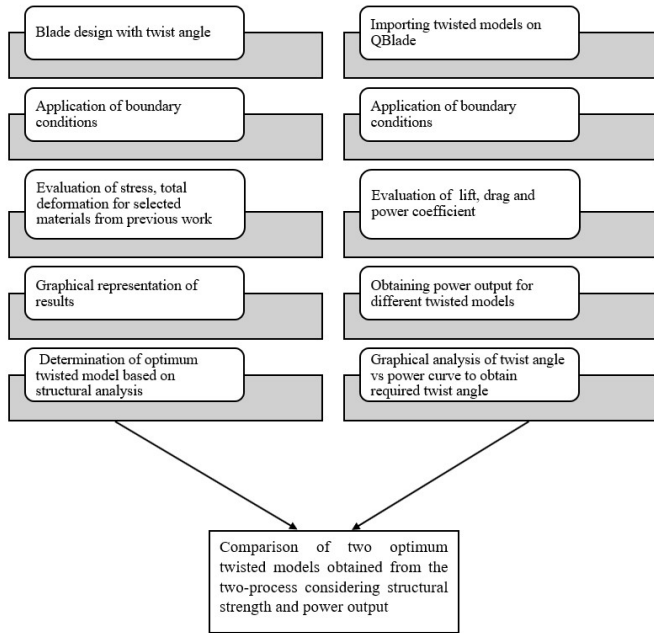
Profile	NACA 2412
Root Chord length	1651 mm
Length of blade	10700 mm
Hub length	1465 mm
Hub Diameter	337.5 mm
Tip Chord length	650 mm
Hub to neck length	1475 mm

Source: Authors.

3. Methodology.

The methodology of this work is divided into two process flow. First process flow represents the determination of optimum twisted model based on the structural integrity and the second process flow represents the optimum twisted model based on power output. Finally, both results are analyzed to find the optimum model which serves both purposes. The process flow of the work is shown in Fig. 4.

Figure 4: Process flow of the work.



Source: Authors.

4. Results and Discussion.

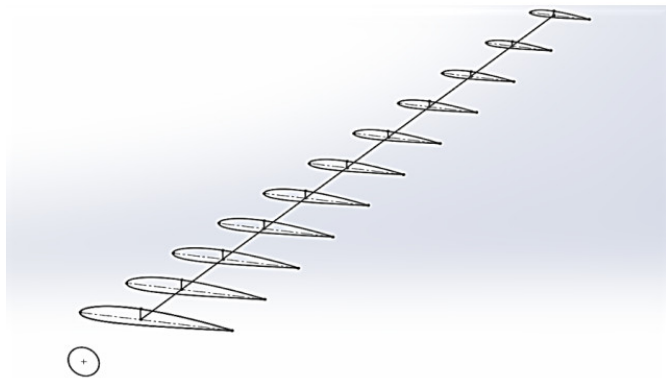
4.1. Determination of Optimum Twist Angle Based on Structural Analysis.

The twist angle is the phase shift between root chord and tip chord of the blade. Wind turbine blades are slightly twisted from root to tip to generate maximum thrust using the wind.

4.1.1. Modeling Twisted Blade.

For modeling twisted blade SolidWorks is used. The whole blade is divided into equally spaced 10 sections depicted in Fig. 5. Each cross section represents NACA 2412 airfoil shape.

Figure 5: Blade sectional divisions.

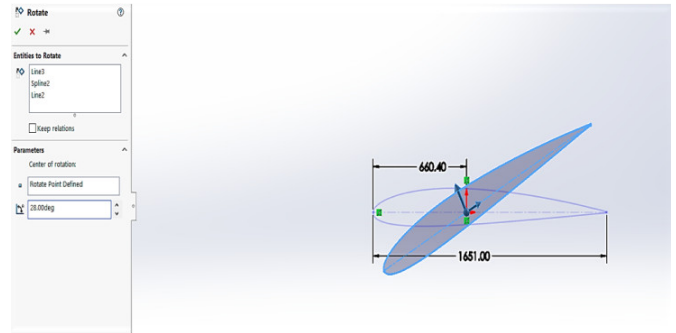


Source: Authors.

The total twist angle of a blade is defined by the difference of twist angle between the root section and the tip section. To

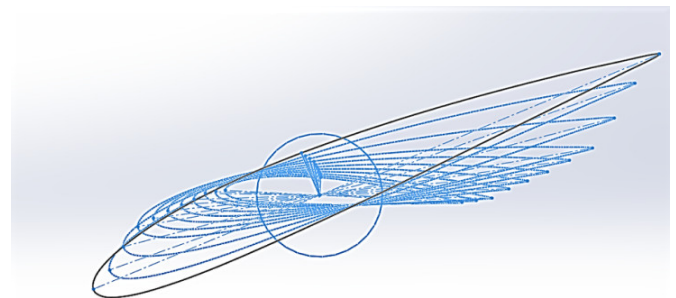
give the blade a certain twist angle, each section is rotated gradually. For example, if a blade with 10-degree twisting is to be modeled, it is to be ensured that the angular difference between root and tip section has to be 10-degree with the intermediate sections having gradual rotation. In this study each section is rotated manually to obtain various combinations of twist angles in the designated blade. Fig. 6 shows the rotation of each individual section. Combining the rotation of each airfoil section, the combined sections are presented in Fig. 7.

Figure 6: Rotation of each section.



Source: Authors.

Figure 7: Total twisted sections.



Source: Authors.

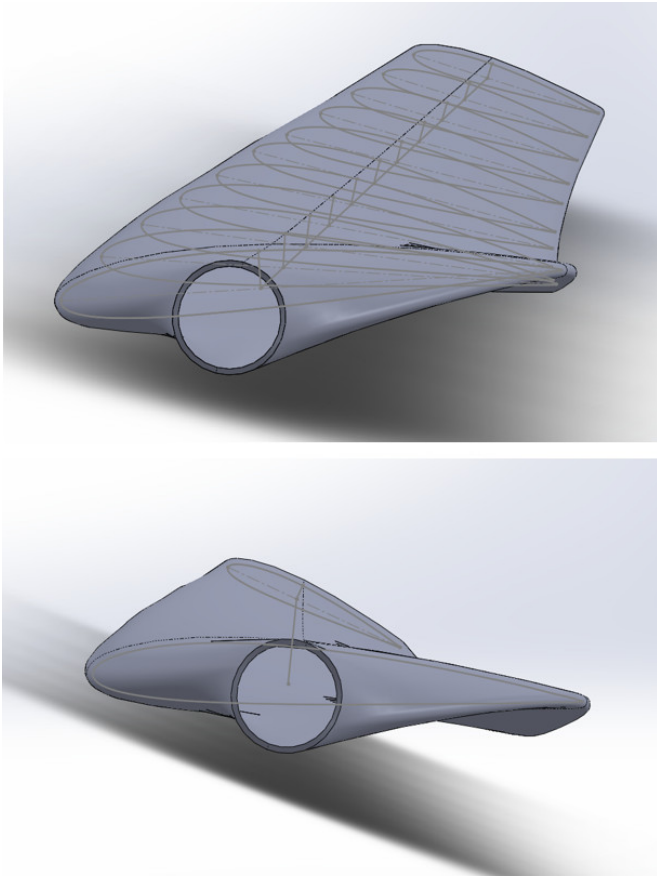
After sectional rotation the whole blade is rendered, and the model is now completed. Similarly, several models of different twisting angles are modeled for further analysis. The twisted blade model is shown in Fig. 8.

4.1.2. Load Application.

Hoque et al. performed a static analysis of wind turbine blades made from various composite materials, demonstrating their advantages over traditional structural steel [3]. Utilizing the NACA 2412 airfoil section, they designed the blade with a zero-twist angle and conducted structural analysis using FEM [3]. Building on the findings from Hoque et al.'s previous work, this study extends the analysis to include twisted blade models.

Loads are applied in the flap wise and edge wise direction. The load equation is represented in the following section,

Figure 8: Twisted blade model.



Source: Authors.

$$F = \pi x \rho x V^2 x D^2 \tag{1}$$

Here,

P = Density = 1.29 Kg/m³.

V = Wind speed = 10 m/s.

D = 30 m.

Applying Equation (1) with the given values, the resulting load is calculated to be 364,554 N, or 364.6 kN.

4.1.3. Boundary Conditions.

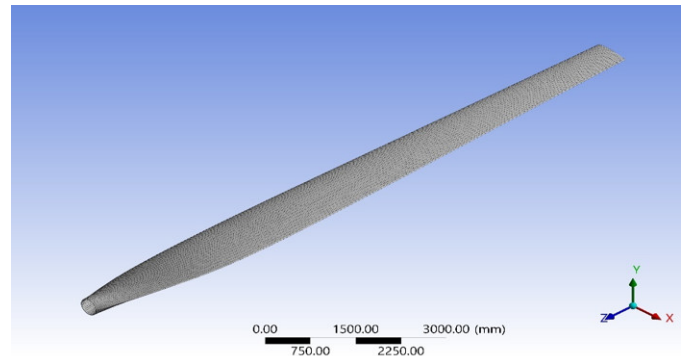
The Hub of the blade is fixed. So, all six degrees of freedom are constrained here. Also, the displacement along X and Z axes are also constrained for the blade and thus only translatory motion is constrained in these directions. This condition was implied so that the blade itself does not deform along the direction of rotation and towards the center.

4.1.4. Meshing.

In this section, several twisted models are analyzed based on previous boundary conditions and loading to determine total deformation and equivalent stress [3]. For each twist angle, four models are analyzed, utilizing Carbon Epoxy UD, E-glass, S-glass, and structural steel. Initially, meshing is performed for

each model. However, if the mesh quality is inadequate, the results will lack accuracy. A good quality mesh is characterized by an aspect ratio below 5 for at least 90 percent of the total elements. Table 2 shows the total number of elements and those with an aspect ratio below 5, enabling the calculation of the aspect ratio percentage. Fortunately, all the models with different twist angles have good quality meshes. Fig. 9 illustrates a fully meshed version of one of the twisted models, while Table 2 provides details on the total number of meshed elements for various models at different twist angles.

Figure 9: Meshing.



Source: Authors.

Table 2: Total number of elements and aspect ratios for different twisted models.

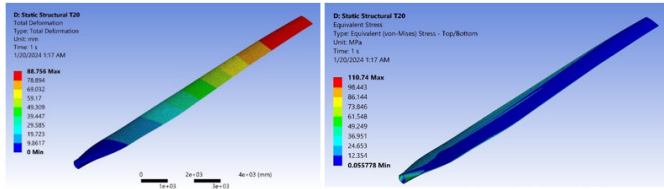
Meshing			
Twist Angle	Total Number of Elements	Aspect ratio Below 5	Percentage
18	17664	17664	100
25	22032	22032	100
10	21930	21930	100
23	23058	23058	100
24.4	13366	13366	100
26	22896	22896	100
20	33924	33924	100
21	14364	14364	100
24	22185	22185	100
21.5	22032	22032	100
22.5	22083	22083	100
22	24192	24192	100

Source: Authors.

4.1.5. Analysis Results.

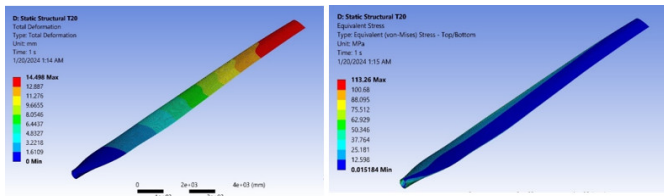
For each twisted model listed in Table 2, stress and deformation are determined using ANSYS Mechanical. Each model is analyzed for four different materials. The materials are selected from a previous work performed by Hoque et al. [3]. These are Carbon Epoxy UD, E-glass, S-glass and structural steel. Fig. 10 to Fig. 13 show the analysis conducted through Ansys Mechanical to find the total deformation and equivalent stress for 20-degree twisted model.

Figure 10: Total deformation and equivalent stress of Epoxy carbon UD for 20-degree twisted model.



Source: Authors.

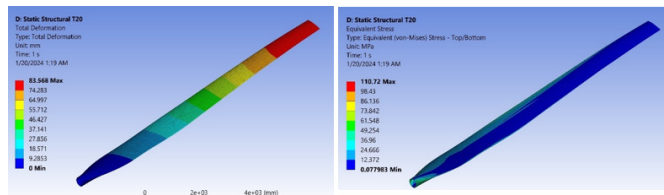
Figure 11: Total deformation and equivalent stress of Structural Steel for 20-degree twisted model.



Source: Authors.

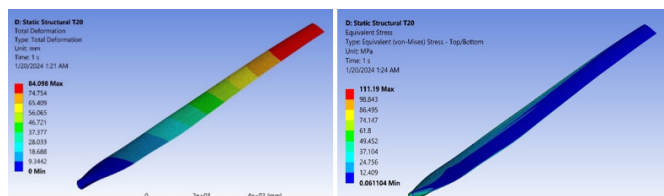
Fig. 10 and Fig. 11 represent the ANSYS Mechanical interface after conduction of the analysis on 20-degree twisted HAWT blade model for Epoxy carbon UD and Structural steel. In Fig. 10, the left analysis shows the total deformation, and the right analysis shows the equivalent stress for the application of static load. Similarly, Fig. 11 represents the total deformation and equivalent stress of the structural steel for the 20-degree twisted model.

Figure 12: Total deformation and equivalent stress of Epoxy E-glass UD for 20-degree twisted model.



Source: Authors.

Figure 13: Total deformation and equivalent stress of Epoxy S-glass UD for 20-degree twisted model.



Source: Authors.

Similarly, Fig. 12 and Fig. 13 display the ANSYS Mechanical interface after analyzing the 20-degree twisted HAWT blade

model for both Epoxy E-glass UD and Epoxy S-glass UD materials. In Fig. 12, the left image shows the total deformation, and the right image shows the equivalent stress of Epoxy E-glass UD under static load. Likewise, Fig. 13 illustrates the total deformation and equivalent stress for the 20-degree twisted model made of Epoxy S-glass UD.

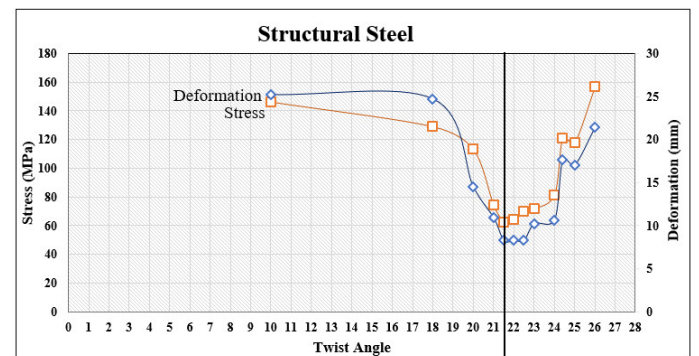
All the analysis results are summarized in Table 3 for better comparison. Table 3 includes results for twisted models ranging from 18 to 26 degrees. Below 18 degrees, the results are significantly poor, and above 26 degrees, there is no considerable improvement. Table 3 presents the stress and total deformation values obtained from the analysis for each twisted model. Additionally, each model is analyzed using four different materials, and all results are displayed for comparison purposes. Table 3 reveals that the deformation and stress values for all materials follow a consistent trend. From a 10-degree twisted blade, both deformation and stress decrease, reaching a minimum between 21.5 and 22 degrees, before rising again after a 24-degree twist. For all materials, the minimum deformation and stress occur between the 21.5 - and 22-degree twisted models.

Table 3: Structural analysis results of wind turbine blade made of different materials.

Twist Angle (°)	Structural Steel		Carbon Epoxy UD		Epoxy E-glass UD		Epoxy S-glass UD	
	Deformation (mm)	Stress (MPa)						
10	25.211	146.41	158.85	149.04	147.65	146.38	148.9	148.01
18	24.721	129.11	143.4	142.37	134.55	148.59	135.26	141.85
20	14.498	113.26	88.756	110.74	83.568	110.72	84.098	111.19
21	10.938	74.423	66.807	73.016	62.914	73.524	63.308	73.654
21.5	8.2779	62.586	51.967	62.836	49.104	62.229	49.233	62.991
22	8.2864	64.473	52.039	63.921	49.198	64.275	49.298	64.289
22.5	8.2976	70.03	52.061	70.247	49.162	69.864	49.307	70.452
23	10.242	71.673	63.887	70.301	60.343	70.321	60.509	70.619
24	10.668	81.593	68.201	83.849	63.737	81.968	64.027	83.31
24.4	17.647	120.98	102.77	116.03	96.568	112.93	97.601	112.06
25	17.038	117.96	105.51	117.67	99.452	116.68	100.01	118.05
26	21.413	156.87	129.8	158.91	121.84	157.52	122.85	158.44

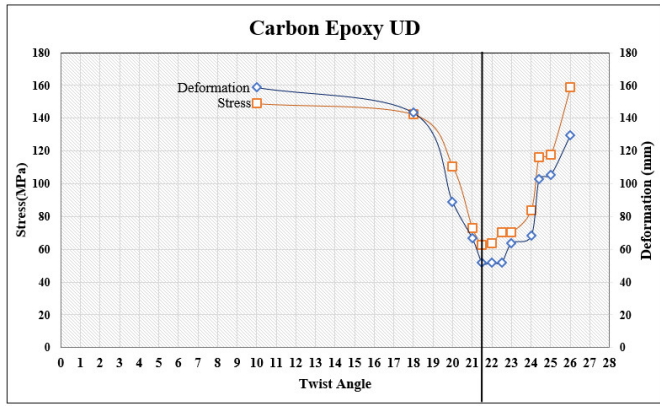
Source: Authors.

Figure 14: Graphical representation of stress and deformation of Structural Steel for various twisted wind turbine models.



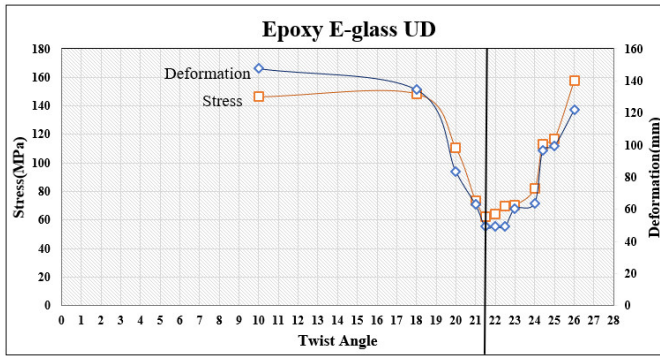
Source: Authors.

Figure 15: Graphical representation of stress and deformation of Carbon Epoxy UD for various twisted wind turbine models.



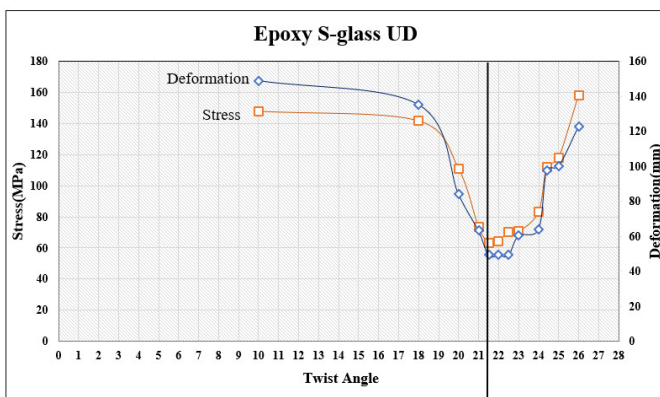
Source: Authors.

Figure 16: Graphical representation of stress and deformation of Epoxy E-glass UD for various twisted wind turbine models.



Source: Authors.

Figure 17: Graphical representation of stress and deformation of Epoxy S-glass UD for various twisted wind turbine models.

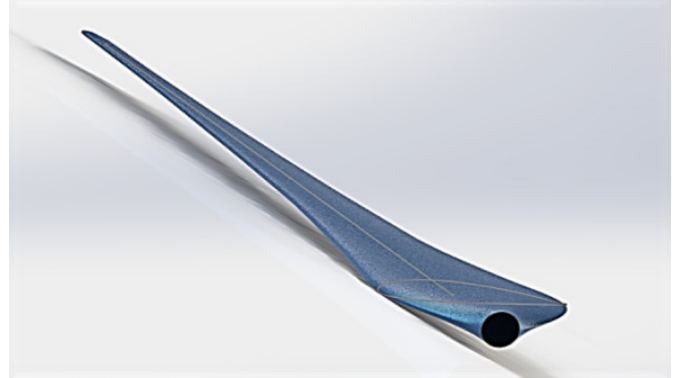


Source: Authors.

Fig. 14 to Fig. 17 present the analysis results for four different materials, with the X-axis illustrating the impact of the twisting angle on deformation and stress. All graphs exhibit a consistent pattern, indicating that the lowest stress and deformation occur at a twisting angle of 21.5 degrees, marked by the black line in each plot.

Therefore, for optimal structural integrity, the ideal twisting angle for the wind turbine blade is 21.5 degrees. The final twisted model is depicted in Fig. 18.

Figure 18: 21.5 degree twisted model.



Source: Authors.

4.2. Determination of Optimum Twist Angle Based on Power Output.

QBlade is a specialized software designed for comprehensive analysis of wind turbines. The software utilizes mathematical formulations based on the Blade Element Momentum (BEM) method. During this phase of the analysis, previously designed models with different twist angles are re-evaluated and analyzed in QBlade to determine power output values [6].

4.2.1. Governing Equation.

Drag coefficient C_D and lift coefficient C_L are required to calculate the drag force (D) and lift force (L) [8],

$$C_D = \frac{D}{0.5\rho AV^2} \tag{2}$$

$$C_L = \frac{L}{0.5\rho AV^2} \tag{3}$$

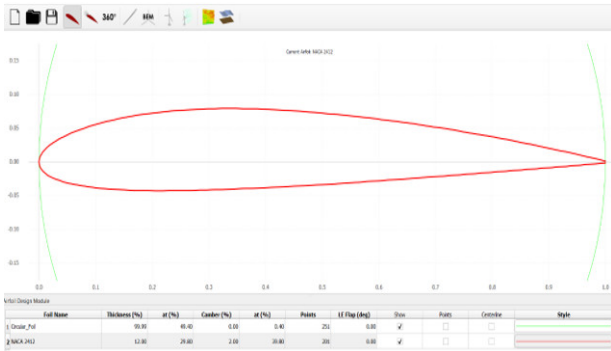
Where ρ represents the density of air, A represents the effective object area, and v represents the wind speed. The Power Coefficient (C_P) is the most crucial factor in selecting a wind turbine. It is defined as the ratio of the actual power generated (P_T) to the overall power of the wind. The wind passes through the blades of a wind turbine when it reaches a specific wind speed (P_0) [8].

$$\frac{P_t}{P_0} = \frac{\frac{1}{4}\rho A(V_1^2 - V_2^2)(V_1 + V_2)}{0.5\rho AV_1^3} \tag{4}$$

4.2.2. Airfoil Generation.

To find the power output the first step is to design the airfoil section. A DAT file of NACA 2412 airfoil section is imported on the QBlade for this purpose. Fig.19 shows the airfoil design section in QBlade interface.

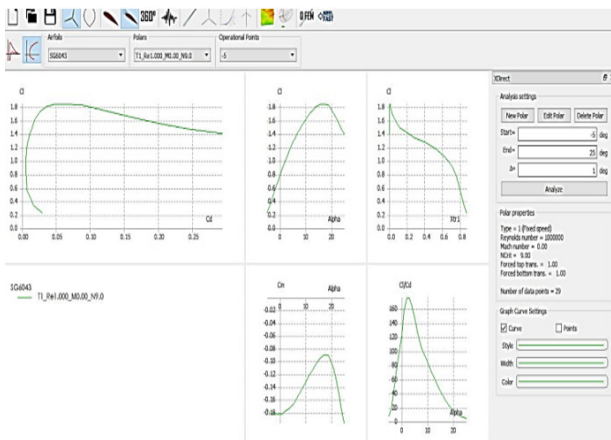
Figure 19: Airfoil generation in QBlade software.



Source: Authors.

Once the appropriate airfoil for the blade has been chosen, the simulation may commence. The XFOIL utilizes a polar perspective to do a direct analysis, which is then employed to establish a fresh analysis. Airfoils with low Reynolds numbers are anticipated to exhibit laminar flow. For this investigation, a Reynolds number of 10^5 is employed. Fig. 20 depicts the relationship between the variables C_L , C_D , and C_L/C_D as they vary with the angle of attack.

Figure 20: C_L , C_D , and C_L/C_D vs. angle of attack.



Source: Authors.

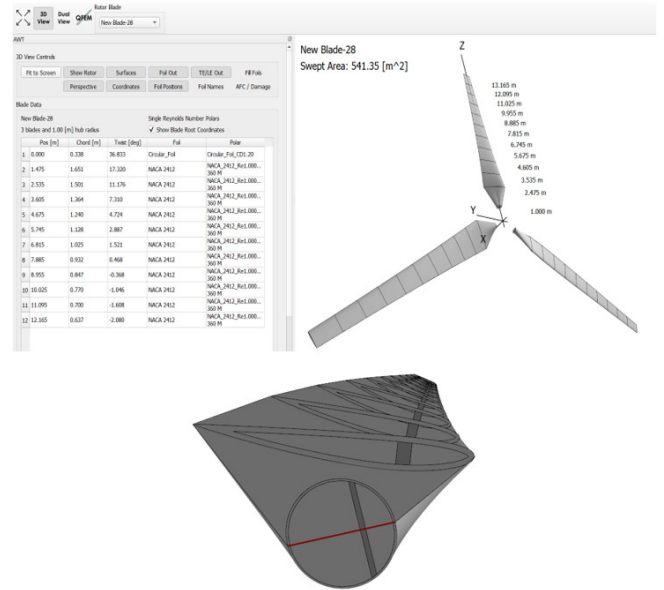
4.2.3. Advance Blade Design.

This study involved the creation of ten segments of HAWT. The chord was defined based on the taper ratio. Fig. 21 shows the maximum thickness of the thread at the centerline, achieved through advanced blade design. The twist angle values for the developed blades were manually input based on the values obtained from the previous analysis in section 5.1.

4.2.4. Analysis Results from QBlade Software.

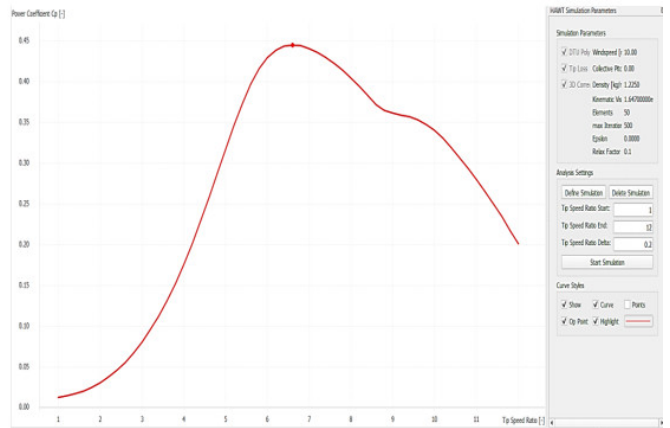
To achieve the Blade Element Momentum Analysis (BEM), rotor (BEM) simulation tab is selected. The resulting simulation is for the power coefficient C_P as shown in Fig. 22. The other important output result such as the power and thrust are recorded by switching to multiparameter BEM simulation. Fig. 23 shows the results for different values of wind speed.

Figure 21: Advanced blade design in QBlade software.



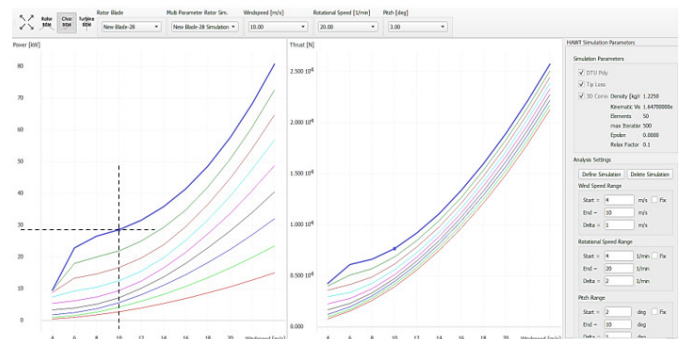
Source: Authors.

Figure 22: Power coefficient C_P vs. tip speed.



Source: Authors.

Figure 23: Power and thrust output results from multiparameter BEM simulation.



Source: Authors.

The initial assumption of this study considers a wind speed of 10 m/s. In Fig. 23, the dotted line indicated the power output for a wind speed of 10 m/s.

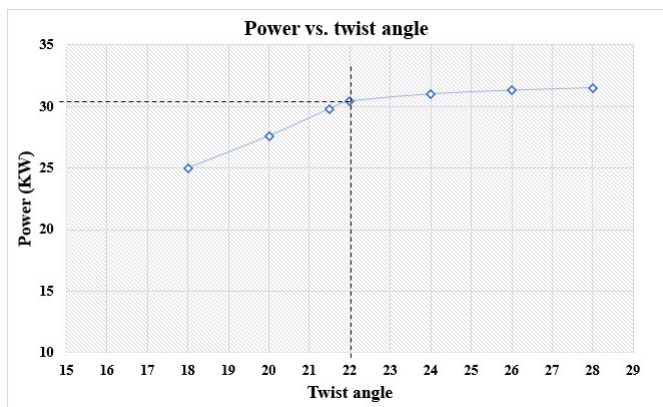
In the same way this analysis is conducted for all the twisted models and their power outputs for 10 m/s are recorded. The power output at 10 m/s wind speed for several twisted models are shown graphically in Fig. 24. The power output at 10 m/s wind speed for different twist angles are highlighted in Table 4.

Table 4: Power output at 10 m/s wind speed for different twist angles.

Twist Angle	Power (KW)
18	25
20	27.6
21.5	29.8
22	30.4
24	31
26	31.3
28	31.5

Source: Authors.

Figure 24: Power output for various twist angle.



Source: Authors.

Fig. 24 indicates that a greater twist angle in the blade enhances power generation. However, while increasing the twist angle may seem beneficial initially for enhancing power output, there are constraints to consider. The twist angle and the structural robustness of the blade exhibit an inverse relationship, necessitating careful consideration to avoid compromising structural integrity. The power curve reveals that power gains begin to level off after reaching a twist angle of around 22 degrees, suggesting this as a critical threshold. Beyond 22 degrees, the incremental increase in power diminishes significantly. Therefore, based on this analysis, the 22-degree twist model is chosen as the optimal configuration for maximizing power output.

5. General Discussion.

The main goal of this study is to optimize the twisting angle of HAWT blades. To achieve this, two separate iterative analysis processes were carried out. The first analysis focused on finding the optimal twist angle for structural stability, resulting in a twist angle of 21.5 degrees. The second analysis aimed at determining the optimal twist angle for maximizing power output, resulting in a twist angle of 22 degrees. Comparing the two results, there is very little difference between the twisting values (21.5 degrees and 22 degrees). The power output for the 21.5-degree twist angle is 29.8 KW, whereas for the 22-degree twist angle, it is 30.4 KW.

If structural integrity is prioritized, the 21.5-degree twist angle is the optimum choice, although there is a minimal decrease in power output, $(30.4 - 29.8) \text{ KW} = 0.6 \text{ KW}$, which can be considered insignificant. On the other hand, if power output is prioritized, the 22-degree twist angle serves the optimum purpose. Graphical analysis from Fig. 14 to Fig. 17 also shows that for the 22-degree twist angle, the increase in stress and deformation is insignificant. Therefore, considering both aspects, an average twist angle of 21.75 degrees can be considered for the optimum choice.

By using SG6043 airfoil section in the analysis of wind turbine blade via QBlade software, Alaskari et al. optimized a horizontal axis wind turbine blade [6]. The chord and twist angle were adjusted using software, resulting in a higher power coefficient compared to the previous configuration. The final blade length was reduced to 1.250 m, and the twist at the root chord was set to 18.3° , which is in close proximity to the current twist angle of 17.32° . However, the twist angle along the blade is 16.9° , lower than the twist angle mentioned in this reference [6]. This variability can be attributed to the utilization of various blade cross-sections, such as NACA 2412 in this study, along with potential differences in blade dimensions. Again, along with these dissimilarities, the wind speed is different and according to Capuzzi et al., the optimum twist angle increases as a function of wind speed [9]. Moreover, in the current QBlade usage, only the twist angle was selected to optimize whereas the chord and blade length were kept constant. Despite these differences, in both cases, the variation in twist angle has led to an improvement in blade performance.

The current analysis is done for a constant wind speed which is 10 m/s. Wang et al. optimized the chord and twist angle distributions by considering blades operating at different Reynold Numbers [4]. The airfoil section chosen was S809 and a MATLAB program was used to address this problem which means a different airfoil section and different approach was used while keeping the wind speed as variable [4]. The optimal blade design in this paper was chosen based on maximizing annual energy production. However, in this study, the selection was based on minimizing stress and deformation as determined by ANSYS structural analysis, prioritizing structural integrity alongside power output from QBlade software. The optimal twist angle in prior research by Wang et al. was nearly 27° [4], exceeding the twist angle selected for the current study. The current analysis involved selecting a twist angle in QBlade software

where power output plateaus; therefore, the maximum power is achieved at a slightly larger twist angle, albeit at the expense of increased stress and the need for additional reinforcement, leading to higher manufacturing costs. Thus, in order to prioritize both structural strength and power output, the twist angle selected for the current study is deemed to be optimal.

Another different way to optimize the blade is the linearization approach which was used by Liu et al. [5]. To optimize chord and twist angle profiles, the DU93W210 airfoil was used, which differs from the airfoil utilized in this study. The best-linearized blade, chosen for its maximum AEP, had a blade root chord of 0.754 m and a blade root twist angle of 17.5° . In this analysis, the optimal blade root twist angle was determined to be 17.32° , while the chord length was significantly different at 1.651 m [5]. This disparity may be attributed to the utilization of different airfoil sections. Nevertheless, both studies concur that twist angle significantly influences blade performance, regardless of the structural analysis method employed.

The study conducted by Hoque et al. compared the performance of wind turbine blades using various composite materials, highlighting their advantages over traditional structural steel materials [3]. The NACA 2412 airfoil section was utilized, and the blade featured a zero-degree twist angle. Furthermore, nodal analysis was performed for each material to pinpoint the areas of highest stress and deformation. The findings revealed that Epoxy E-glass UD, Epoxy S-glass UD, and Epoxy Carbon UD (230 GPa) surpassed other materials in performance. This research extends the work of Hoque et al. by introducing blade optimization, which holds greater practical significance compared to employing a blade with zero-twist angle. Implementing the same materials in a modified twisted blade resulted in improved stress and deformation values, rendering them more suitable for practical applications.

Conclusions.

This paper outlines the optimization of the twist angle for a horizontal axis wind turbine (HAWT) blade utilizing a NACA 2412 profile. This study builds upon a previous investigation, which focused on identifying suitable materials for ensuring adequate structural strength in a simple HAWT model with a zero-twist angle. The current study proposes an approach to twist angle optimization that takes into account both the structural integrity and power output of the wind turbine blade.

An iterative design process was carried out to generate more practical models with twist angles ranging from 5 to 30 degrees. Finite element analysis, conducted using ANSYS Mechanical under static load, demonstrated that the model with a twist angle of 21.5 degrees exhibited superior structural strength with lower stress and deformation. The structural materials were selected based on findings from the previous study [3]. Additionally, an analysis in QBlade software was performed to determine the power output of each designed twisted model, taking into consideration the airfoil profile of NACA 2412 and parameters such as the drag coefficient and lift coefficient. The power output at a wind speed of 10 m/s was recorded and graphically

represented for all models, revealing that the 22-degree twisted model yielded the optimal power output.

The results show that there is very little difference between the twist angles of 21.5 degrees and 22 degrees. At a 21.5-degree twist angle, the power output is 29.8 kW, whereas at a 22-degree twist angle, it is 30.4 kW. Considering structural integrity as a priority, the 21.5-degree twist angle is optimal, despite a slight decrease in power output of 0.6 kW, which is negligible. However, if maximizing power output is the goal, then the 22-degree twist angle is preferable. The analysis indicates that the increase in stress and deformation at the 22-degree twist angle is insignificant. Thus, taking both factors into account, an average twist angle of 21.75 degrees is considered the optimal choice.

Acknowledgements.

The authors extend heartfelt thanks to all those who have offered valuable support at different stages of this research work, both directly and indirectly. Special recognition is given to the UGC HEQEP Sub-Project "Strengthening the Research Capabilities and Experimental Facilities in the Field of Marine Structure" (CP#3131), which has played a crucial role in improving the simulation lab facilities. The authors gratefully acknowledge the financial support provided by the Research and Innovation Center for Science and Engineering (RISE) at BUET, under the research project titled "Analysis of Wind Turbine Blade Using Finite Element Method" (Grant ID: S2023-03-096). Additionally, gratitude is expressed to the "Basic Research Grant" for providing financial support to enhance the research endeavors.

References.

- [1] Khaled, M., Ibrahim, M.M., Hamed, H.E.A. and Gawad, A.F.A., "Aerodynamic Design and Blade Angle Analysis of a Small Horizontal-Axis Wind Turbine," *American Journal of Modern Energy*, vol. 3, no. 2, pp. 23-37, 2017.
- [2] Mouhsine, S.E., Oukassou, K., Ichenial, M.M., Kharbouch, B. and Hajraoui, A., "Aerodynamics and structural analysis of wind turbine blade," *Procedia Manufacturing*, vol. 22, pp. 747-756, 2018.
- [3] Hoque, K.N., Chowdhury, S.A. and Haque, S.A., "Structural analysis of wind turbine blade by using finite element method," *JOURNAL OF MARITIME RESEARCH*, vol. 20, no. 3, pp. 224-239, 2023.
- [4] Wang, L., Tang, X. and Liu, X., "Optimized chord and twist angle distributions of wind turbine blade considering Reynolds number effects," in *International Conference on Wind Energy: Materials, Engineering and Policies (WEMEP)*, India, 2012.
- [5] Liu, X., Wang, L. and Tang, X., "Optimized linearization of chord and twist angle profiles for fixed-pitch fixed-speed wind turbine blades," *Renewable Energy*, vol. 57, pp. 111-119, September 2013.
- [6] Alaskari, M., Abdullah, O. and Majeed, M.H., "Analysis of Wind Turbine Using QBlade Software," *IOP Conference*

Series: Materials Science and Engineering, vol. 518, no. 3, p. 032020, 2019.

[7] Mendez, J. and Greiner, D., "Wind blade chord and twist angle optimization by using genetic algorithms," in Proceedings of the Fifth International Conference on Engineering Computational Technology, Las Palmas de Gran Canaria, Spain, 2006.

[8] Twidell, J., *Renewable Energy Resources* (4th ed.), London: Routledge, 2021.

[9] Capuzzi, M., Pirrera, A. and Weaver, P.M. , "A novel adaptive blade concept for large-scale wind turbines. Part I: Aeroelastic behaviour," *Energy*, vol. 73, pp. 15-24, 14 August 2014.